[5]J. Hubbard and N. W. Dalton, J. Phys. C 1, 1637 (1968).
[6]R. L. Jacobs, J. Phys. C 1, 492 (1968).
[7]D. G. Pettifor, J. Phys. C 2, 1051 (1969).
[8]D. M. Hum and K. C. Wong, J. Phys. C 2, 833 (1969).
[9]J. Hubbard, J. Phys. C 2, 1222 (1969).
[10]J. M. Ziman, Solid State Phys. 26, 1 (1971).
[11]F. M. Mueller, A. J. Freeman, J. O. Dimmock, and A. M. Furdyna, Phys. Rev. B 1, 4617 (1970).
[12]J. M. Ziman, Proc. Phys. Soc. (London) 86, 337 (1965).
[13]J. Korringa, Physica 13, 392 (1947).
[14]W. Kohn and N. Rostoker, Phys. Rev. 94, 1111 (1954).
[15]F. Herman and S. Skillman, *Atomic Structure Calculations* (Prentice-Hall, Englewood Cliffs, N. J., 1963).
[16]T. L. Loucks, *Augmented Plane Wave Method* (Benjamin, New York, 1967).

PHYSICAL REVIEW B VOLUME 7, NUMBER 4 15 FEBRUARY 1973

Thermal Resistivity of Potassium between 1.5 and 15 K†

R. S. Newrock and B. W. Maxfield*
Laboratory of Atomic and Solid State Physics, Cornell University, Ithaca, New York 14850
(Received 31 July 1972)

The thermal resistivity of single-crystal and polycrystalline potassium specimens having residual-resistance ratios between 195 and 6500 has been measured between 1.5 and 15 K. It is found that theoretical calculations based on semiclassical ideas are in reasonably good agreement with the experimental data, particularly for the more impure specimens at low temperatures. The role of umklapp scattering is clearly evident. Although the umklapp processes can contribute as much as 50% to the total thermal resistivity, the simple expression $W=A/T+BT^2$, obtained by only considering normal scattering, describes the results remarkably well up to about 10 K. Depending upon the purity, the values of B ranged from 2.38×10^{-3} cm/W to 1.53×10^{-3} cm/W, indicating a deviation from Matthiessen's rule of about 50%. The magnitude of the calculated thermal resistivity is very near the experimental result for impure specimens but the calculated values are too high for the purer specimens. It is shown that when impurity scattering is dominant, a variational calculation of the electron-phonon thermal resistance should be quite accurate. In pure specimens the calculations are not expected to be nearly as good; reasons for this are discussed. At high temperatures, above 6 to 8 K, the theoretical temperature dependence is in considerable disagreement with the experimental results. Deviations from Matthiessen's rule, as well as other possible reasons for this discrepancy, are discussed. Our data are in qualitative agreement with that of MacDonald, White, and Woods; however, contrary to the observations of Stauder and Mielczarek, we observe no anomalous behavior in the thermal conductivity of potassium. Reasons for the differences between our results and those of Stauder and Mielczarek are presented and discussed. We conclude that the thermal resistance of potassium can be understood very well within the framework of existing theoretical work. In specimens of low and intermediate purity the contribution of lattice thermal conduction can be appreciable and should be taken into account when making comparisons with theory.

I. INTRODUCTION

In recent years there have been many measurements of the various transport properties of the alkali metals. Much of this work has been on potassium,[1–7] which is known to have a Fermi surface spherical to about one part in a thousand.[8,9] In addition, it can be obtained with high purity and does not have the complicating feature of a martensitic phase transformation that exists in lithium and sodium. The high reactivity and other handling problems have made experimental work quite difficult; only recently, for instance, has sufficiently good data been obtained to allow a detailed comparison of the measured electrical resistivity with theory.[1,3] In zero magnetic field, the electrical resistivity can be explained very well by semiclassical transport theories provided electron-phonon umklapp scattering is taken into account. On the other hand, the high-field magnetoresistance of potassium, which increases linearly with applied magnetic field over a wide field range,[2,4,6,7] has proven difficult to explain on a semiclassical basis.

To further elucidate the transport properties of potassium it was decided to investigate the thermal and magnetothermal resistivity to determine the possible existence of differences similar to those observed for the electrical resistivity. This paper reports our zero-magnetic-field thermal resistivity measurements. Single-crystal and polycrystalline potassium specimens have been measured between 1.5 and 15 K in specimens having residual-resistance ratios ranging from 195 to

6500.

There are only two other measurements of the low-temperature thermal resistance of potassium. The first by MacDonald, White, and Woods[10] was done on specimens encapsulated in glass capillaries. In addition to possible problems arising from differential thermal contraction, their data are not sufficiently extensive to permit detailed comparison with recent theoretical calculations. An anomalous behavior which is difficult to explain on any fundamental basis is observed in the second set of measurements.[11] Section II contains a detailed discussion of the sample preparation and mounting procedures. Section III describes the results and makes comparisons to other work. In particular, the role of umklapp scattering in the thermal resistivity is discussed, the lattice conductivity is shown to be of importance even in reasonably pure samples, and fairly large deviations from Matthiessen's rule are noted. Some concluding remarks are contained in Sec. IV.

II. EXPERIMENTAL DETAILS

For any particular transport property of potassium, there are often a variety of results reported in the literature. Most of the differences can be attributed to probe effects and to problems related to sample preparation and mounting. In view of this and the previously reported anomalous thermal resistivity of potassium,[11] we feel that it is necessary to describe the experimental and sample preparation techniques in more than the usual detail. The following subsections explain the mounting procedures, sample preparation and details of the apparatus as well as the methods of data acquisition and analysis.

A. Sample Preparation

Potassium ranging from 99 to 99.95% nominal purity was used; the least pure samples were made by alloying pure potassium with pure sodium. Potassium, in the glass ampules supplied by the manufacturer, was melted under vacuum into Pyrex tubes that had been coated with dry paraffin oil. While in the liquid state, the metal was outgassed in a vacuum of better than 10^{-5} Torr for at least 24 h. If a single crystal was desired, the oven temperature was slowly lowered while an auxiliary heater maintained a thermal gradient; this procedure generally resulted in the formation of large (2×10 cm) single crystals.

For some of the polycrystalline samples, pieces were cut from the large boules, etched in xylene containing 2% secondary butyl alcohol, coated with dry paraffin oil, and pressed into 1-mm-thick plates using a stainless-steel sample press. From these pressed plates, samples were cut to size with a razor blade. For other specimens, potassium prepared as described above was extruded using a 1×3-mm die. The single-crystal samples were either string cut from the large boules or grown between glass plates on a hot plate. After fabrication, all samples were etched and placed in a vacuum dessicator filled with dry paraffin oil. The samples were then allowed to anneal at room temperature for at least 24 h before being measured.

Table I lists the physical characteristics of the samples. Owing to the rapid deterioration of the surface upon exposure to air (and the subsequent need for etching), and the fact that the samples cannot be measured accurately after forming, the cross-sectional area of the samples is only accurate to 5%.

B. Cryostat

A schematic view of the cryostat is shown in Fig. 1. All of the salient features are presented in the caption; however, a few points are worth further elaboration. H2 is the heater used to establish the thermal gradient. The former is made of phosphor

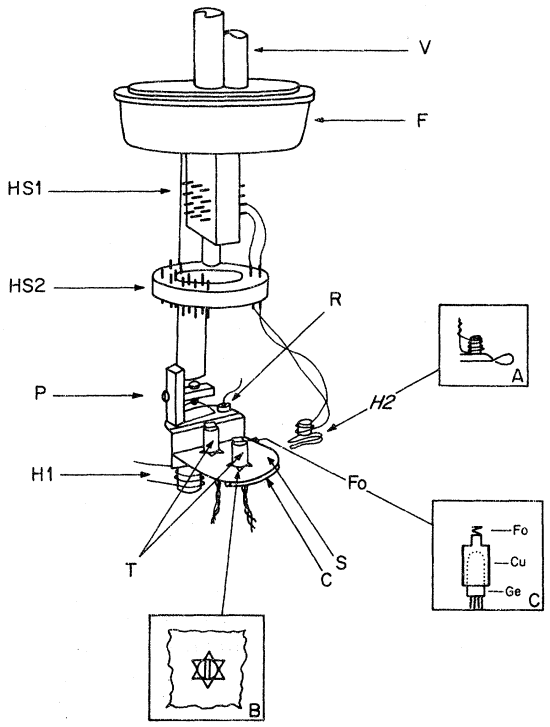

FIG. 1. Cryostat: HS1 and HS2 are heat stations, HS1 is connected directly to the bath; S is a stainless-steel platform with a copper rod C around the perimeter; T are the measuring thermometers and R is the control thermometer; Fo is a pleated copper foil, Cu is the thermometer holder and Ge is the germanium resistance thermometer; *P* is a small press; F is a tapered flange and V are the vacuum lines.

TABLE I. Physical characteristics of samples.

Sample[a]	$A^b=(WT)_{T=0}$ (10^{-2} cm K^2/W)	B^b (10^{-3} cm/W)	RRR[c]	Type	Width[d] (mm)	Thickness[d] (mm)
K-9	4.8	1.53	6130	poly.	7.0	1.0
K-10	6.6	1.65	4455	poly.	7.0	1.0
K-11	16.5	2.23	1780	poly.	3.5	1.0
K-12	6.8	1.72	4325	poly.	3.0	1.0
K-13	5.5	1.73	5345	poly.	3.0	1.0
K-14	7.1	1.94	4140	single	5.0	1.0
K-15	26.8	2.35	1095	single	3.0	1.5
K-16	151.2	2.38	195	poly.	3.0	1.0
K-17	4.5	1.80	6535	poly.	3.0	1.0

[a]Our potassium was purchased from MSA Corp., Evans City, Pa.

[b]The coefficients A and B are obtained by fitting the data to $W=A/T+BT^2$ as described in the text.

[c]The residual-resistivity ratio (RRR) is determined using the Wiedemann–Franz law; see Ref. 23.

[d]The thickness measurements were accurate to better than ±0.05 mm while the width measurements are accurate to about ±0.1 mm.

bronze twisted into a tweezerlike shape (see inset A). The heater is wound on a cylinder of copper foil and soldered to this former; such an arrangement allows the heater to be attached quickly and firmly to the potassium. It also has the advantage that heat flows into the sample from both sides. Flange F is tapered and mates with a corresponding flange on the vacuum can. When the mating surfaces are coated with a thin film of silicon grease,[12] a seal that is leak tight to superfluid helium can be made in a few seconds. This enables the air to be pumped from around the sample before the potassium surfaces can deteriorate.

The specimen platform was made from 5-mil stainless-steel shim stock. Six-pointed star-shaped holes (see Fig. 1, inset B) were spark machined into the platform to support the measuring thermometers. This was necessary because it is very difficult to attach anything directly to potassium at room temperature. Most glues and varnishes will react with potassium and it is too soft to withstand the pressure of mechanical clamps. In this configuration, the thermometers serve as supports for the sample and are separated by a high thermal resistance.

The thermometers are calibrated germanium resistors mounted in small copper holders with GE-7031 varnish. These copper holders, which have flat upper surfaces, are inserted into the stars in the platform. To the flat copper surface is attached a 1-mil-thick accordian-folded copper foil (see Fig. 1, inset C). The sample is connected to these foils which allow for the differential contraction between the sample and the stainless-steel platform. This avoids introducing strains into the sample when the apparatus is cooled. To ensure thermal isolation, the thermometers are attached to the heat station pins with approximately 3 Ω of copper and Evanohm wire. (The leakage power is therefore about 0.03 μW/deg temperature difference.) A copper bar is attached as shown, to the perimeter of the stainless-steel platform, to aid it in reaching thermal equilibrium. Attached to the heat post is a press that is used to obtain a small thermal resistance between the helium bath and the sample. An ac Wheatstone bridge and a carbon-resistance thermom eter attached to the copper portion of the platform near the press are used to control the sample temperature through heater H1. The specimen temperature could be stabilized to about 0.05 mK.

The data acquisition system used is essentially the same as described by Stephan and Maxfield.[13] Briefly, it consists of a scanner, a digital voltmeter (DVM), and both printed and punched paper-tape output. Using a 25-Hz current phase-locked to the DVM clock frequency, both the thermometer current and potential drop are measured using a four-terminal configuration. The acquisition system puts the thermometer currents and voltages, the heater current and voltage, and all other pertinent information onto the punched paper tape for computer analysis. This system works very well for temperatures greater than 2 K. However, below this temperature, noise in the scanner stepping switch made accurate measurements of the temperatures impossible[14]; at the lower temperatures the scanner was manually stepped and the system allowed to stabilize after each step.

C. Sample Mounting Procedure

The annealed sample was carefully removed from the paraffin oil and etched slightly. It was then dipped in dry Dow-Corning DC-200 fluid[15] (200 cS viscosity), the excess fluid being allowed to drain off leaving a very thin coating of fluid that served to retard surface deterioration. A drop of very viscous DC-200 fluid (60 000 cS) was placed on the ends of the pleated copper foils attached to the thermome-

ters, the sample was placed on top of the foils with one end on the heat post, and a small pressure applied via the press. The DC-200 fluid, when frozen, adheres very well to the potassium and provides an adequate thermal link between the potassium and the thermometers and heater. Several other oils and greases were tried with little success[16]; they all tended to crack at liquid-nitrogen temperature.

The thermal resistance of a typical DC-200 thermal joint was measured to about 450 K/W at 6 K. At this temperature both the power dissipated in the thermometers and the maximum possible heat leak through the thermometer leads was always less than 0.1 μW. A heat current of 0.1 μW through such a foil-DC-200 joint will give a temperature difference of approximately 0.05 mK, a negligible error for the temperature gradients that could be used above 3 K. At low temperatures the resistance of the joint increases but there is a corresponding decrease in both the power dissipated in the thermometers and in the thermometer lead heat conduction. In practice, errors attributable to this thermal joint were negligible above 1.5 K. For comparison purposes, the thermal resistance of a 1-mil-thick layer of GE-7031 varnish of similar cross sections is approximately 50 K/W.[17]

After placing the hot heater onto the sample, the vacuum can was put in place and the cryostat evacuated. The time between removal of the sample from the DC-200 fluid and the end of the mounting procedure was between 60 and 90 sec; in addition it took about 2 min to evacuate the system to 100 μ. Upon opening the system, there was always some oxidation present on the surface of the sample although there was seldom any in the vicinity of the thermometers.

After evacuation, the cryostat was cooled slowly to liquid-nitrogen temperatures. All of the samples were *slow cooled*,[1] meaning that it took from $\frac{1}{2}$ to 2 h to reach 77 K. Using such a procedure, it has been shown that, in very pure potassium, the electrical residual-resistivity ratio can be doubled over that obtainable by quenching the sample from 300 to 77 K.[1]

D. Calibration, Testing, and Measurements Procedure

The germanium resistance thermometers used in this experiment was calibrated against a commerical standard.[18] For calibration, all thermometers were placed in a large copper block that was attached to the platform of the cryostat described previously. The resistance of all thermometers was determined at many temperatures between 1.2 and 20 K. A curve-fitting routine using Chebyschev polynomials gave calculated temperatures that matched the measured ones to within 1 mK below 5 K and within 4 mK above 5 K. Below 4.2 K, the thermometer calibration was also checked against the vapor pressure of liquid helium.

The thermal resistivity data are taken in the following manner: Power is applied to the cold heater H1 until the cold thermometer resistance indicates that the desired temperature has been reached; the resistance of each thermometer is then measured. This gives the zero-heat-current temperature difference and acts as a correction for small calibration errors and heat leaks into the thermometers. Power is next applied to the hot heater H2 while power in the cold heater is adjusted to bring the cold thermometer back to the correct temperature. Again, the resistance of each thermometer is measured. The thermal resistance is calculated from the hot heater power and the true temperature difference. The gradients used were less than 50 mK below 4.2 K, less than 100 mK between 4.2 and 8 K, and less than 200 mK above 8 K.

Because of the relatively poor thermal conductance between the thermometer and the specimen, self-heating must be kept to an absolute mimimum. To ascertain whether these quantities had any undesirable effects upon our measurements and to test the apparatus in general, several runs were performed on indium specimens following essentially the same mounting procedure as used for the potassium. The temperature dependence of the thermal resistivity of a typical indium specimen is shown in Fig. 2 plotted as WT vs T^3 [see Eq. (14)]. Results for other specimens as well as those of other workers are given in Table II. Our results are in good agreement with literature values. The thermal resistivity showed no dependence upon either heater or thermometer power within the experimental range of these parameters.

III. RESULTS AND DISCUSSION

The temperature dependence of the thermal resistivity W of potassium is shown in Figs. 3–9. To facilitate comparison with recent theoretical calculations, Figs. 3 and 4 show W_T/T^2 as a function of the temperature, where $W_T T = WT - (WT)_{T=0}$ and

TABLE II. Coefficients A and B for several indium specimens used in this study as well as the results obtained by others.

	A[a](cm K^2/W)	B[a](10^{-3} cm/W)
Hulm[b]	0.138	1.89
In A	0.014	1.64
In B	0.009	1.51
In C	0.0085	1.41
Jones and Toxen[c]	0.0034	1.11

[a] A and B are coefficients obtained by fitting the data to $W = A/T + BT^2$.

[b] J. K. Hulm, Proc. Roy. Soc. A204, 98 (1950).

[c] R. E. Jones and A. N. Toxen, Phys. Rev. 120, 1167 (1960).

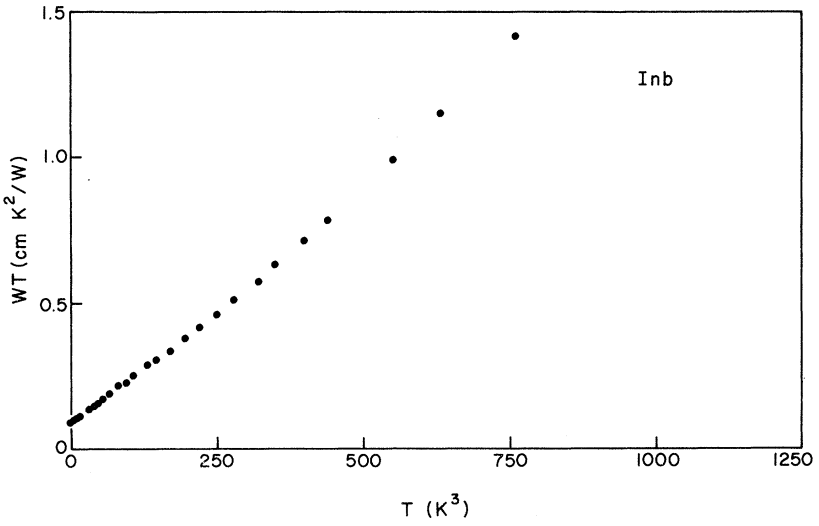

FIG. 2. Thermal resistivity of indium multiplied by the temperature as a function of T^3; indium was measured as a check on the measurement procedure.

is the experimentally determined temperature-dependent portion of WT. A smooth extrapolation to zero temperature of WT as a function of T^3 is used to obtain the temperature-independent portion of WT; the zero-temperature intercept is then subtracted from each of the measured points to obtain W_T. The data in Figs. 3 and 4 are representative of all samples that were measured; the larger amount of scatter in the low-temperature data arises from problems inherent in subtracting two nearly equal numbers. Data plotted in this manner emphasize deviations from the simple Bloch theory of thermal conductivity. If only normal electron-phonon scattering were important, then the thermal resistivity should increase as T^2 for $T \leq 0.1\Theta_D$, where Θ_D is the Debye temperature ($\Theta_D \approx 90$ K for potassium[19]);

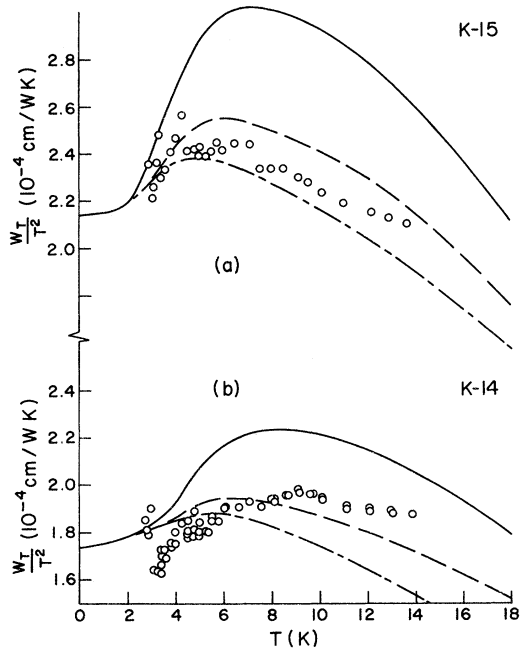

FIG. 3. Temperature dependence of W_T/T^2, where $W_T T = WT - (WT)_{T=0}$ (see text) for (a) sample K-15, (b) sample K-14. The curves are theoretical values calculated by Ekin using different pseudopotentials: solid line, Bardeen pseudopotential; broken line, Lee–Falicov pseudopotential; double broken line, Ashcroft pseudopotential. The relaxation time trial function [Eq. (1)] was used for the calculations in (a) and the corrected trial function [Eq. (2)] for the calculations in (b).

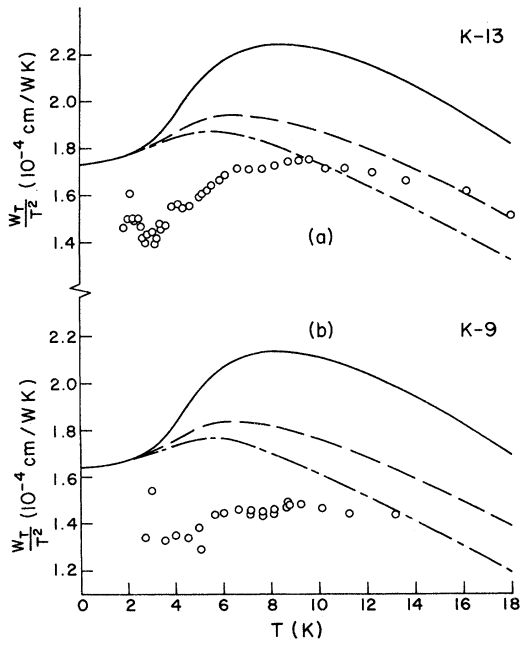

FIG. 4. Temperature dependence of W_T/T^2 for (a) sample K-13, and (b) sample K-9. The curves are the same as shown in Fig. 3(b).

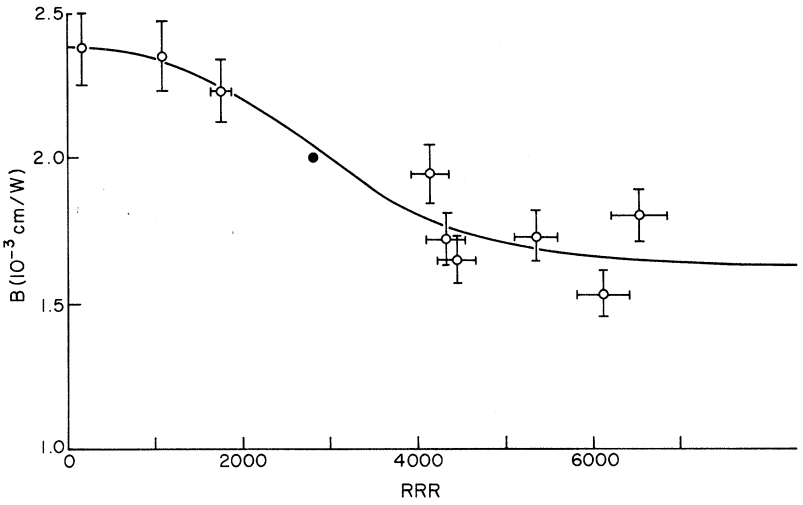

FIG. 5. Coefficient B [see Eq. (14)] as a function of the RRR. The open circles are data from this work, the closed circle is from Ref. 30.

such behavior would correspond to a straight, horizontal line in Figs. 3 and 4.

The solid and dashed curves shown in Figs. 3 and 4 are theoretical curves calculated by Ekin[20] using the Kohler variational method; as indicated in the figure captions, each curve corresponds to a different pseudopotential. Electron-phonon umklapp processes are specifically included in the calculation and appropriate measured parameters for potassium (such as the phonon spectrum and lattice constant) were used. Also, the phonon system is assumed to be in equilibrium; that is, no phonon drag effects are included. The theoretical curves in Fig. 3(a) were calculated using the trial function

$$\phi = \vec{k} \cdot \hat{u}(\epsilon - \mu), \tag{1}$$

where $\vec{k}$ is the electron wave vector, $\hat{u}$ is a unit vector in the direction of the thermal gradient, μ is the chemical potential, and ϵ is the electron energy. This trial function is the exact solution to the linearized Boltzmann equation in the relaxation-time approximation. No adjustable parameters were used in calculating the theoretical curves (see Ref. 20). In Figs. 3(b) and 4, which show results for intermediate and high-purity samples, the calculated values were obtained using a corrected trial function

$$\phi = \vec{k} \cdot \hat{u}(\epsilon - \mu)\{1 + a(T)[(\epsilon - \mu)/k_B T]^2\}, \tag{2}$$

where $a(T)$ is a variational parameter. Qualitatively, the calculations agree very well with the data. The definite "hump" in the data is due to umklapp scattering, and corresponds to large wave-vector phonons being frozen out of the phonon distri-

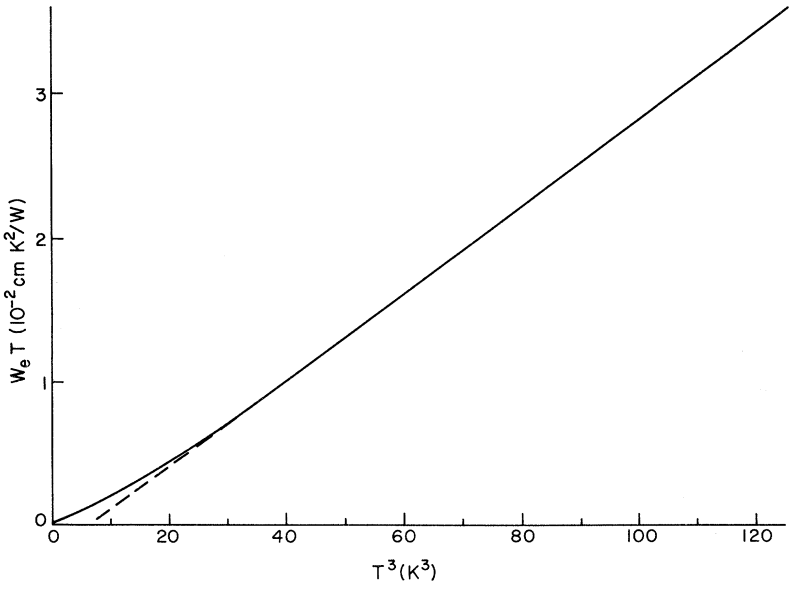

FIG. 6. Calculated thermal resistance given by the solid curve in Fig. 3(a) replotted as WT vs T^3. The dashed line is an extrapolation of the linear high-temperature region.

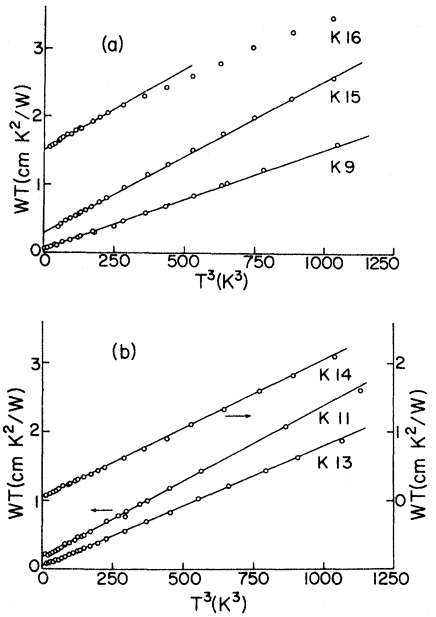

FIG. 7. Measured thermal resistance of potassium times the temperature as a function of T^3; (a) for samples K-9, K-15, and K-16; and (b) for samples K-11, K-13, and K-14.

bution at the lower temperatures. As the temperature increases, larger wave-vector phonons are excited, increasing the amount of umklapp scattering and thereby increasing W.

For the very impure samples, the quantitative agreement between our measurements and the calculated values is very good, even though a very simple trial function is used to calculate the temperature-dependent portion of the electronic thermal resistivity. In the treatment that follows we show explicitly that if a particular scattering mechanism is dominant and if that mechanism can be described by a relaxation time, then the relaxation-time trial function can be used to obtain the temperature dependence of those scattering mechanisms not describable by a relaxation time.[21]

The electrical and electronic thermal currents in a metal are given, respectively, by

$$\vec{J}_e = \overleftrightarrow{L}_{EE} \cdot \vec{E} + \overleftrightarrow{L}_{ET} \cdot \vec{\nabla} T, \tag{3}$$

$$\vec{J}_Q = \overleftrightarrow{L}_{TE} \cdot \vec{E} + \overleftrightarrow{L}_{ET} \cdot \vec{\nabla} T, \tag{4}$$

where the L_{ij} are elements of the thermoelectric tensor.[22] In zero magnetic field the tensors reduce to scalars for materials having cubic symmetry. Therefore, from Eqs. (3) and (4), it follows that

$$\sigma = L_{EE}, \quad \kappa_e = -(L_{TT} - L_{ET} L_{TE}/L_{EE}),$$

$$Q = -L_{ET}/L_{EE},$$

where σ, κ_e, and Q are the electrical conductivity, electronic thermal conductivity, and the thermopower, respectively. Using the Onsager relation $L_{ET} = -L_{TE}/T$, one obtains

$$\kappa_e = -(L_{TT} + Q^2 T\sigma). \tag{5}$$

Using the free-electron theory of metals, an order-of-magnitude estimate can be obtained for the second term in the bracket of Eq. (5). Taking a Fermi energy of 2.1 eV for potassium gives $Q \approx 60$ nV/K at 5 K.[22] Thus, for potassium having a residual-resistivity ratio[23] of 100 (very impure), one obtains $Q^2 T\sigma \sim 3 \times 10^{-7}$ W/cm K. For potassium of this purity, κ_e is typically greater than 1 W/cm K, so thermoelectric effects can be ignored. Hence we have $\kappa_e = -L_{TT}$ and $J_Q = \kappa_e \nabla T$.

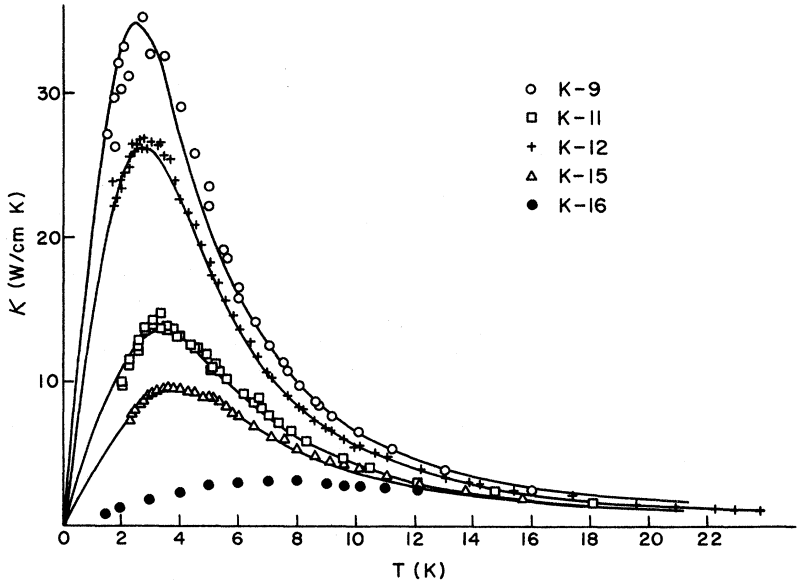

FIG. 8. Thermal conductivity κ as a function of temperature for potassium samples ranging in purity from RRR = 6000 to RRR = 195. The curves are calculated from $1/\kappa = A/T + BT^2$. [See Eq. (14) and Table I.]

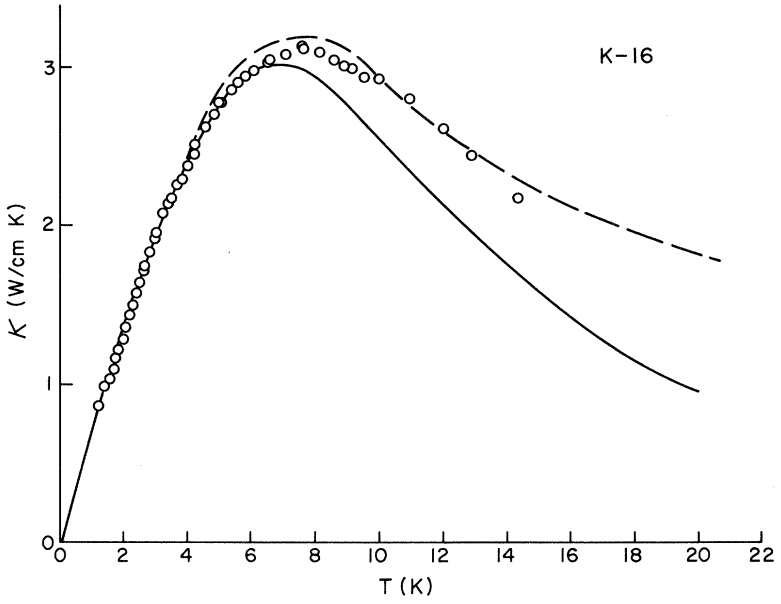

FIG. 9. Thermal conductivity as a function of temperature for the lowest purity sample K-16. The solid line is calculated from $1/\kappa = A/T + BT^2$ [see Eq. (14) and Table I]. As described in the text, the broken line includes the lattice thermal conductivity in the calculated values.

The thermal current can be written

$$\vec{J}_Q = (1/4\pi^3)\int d\vec{k}\, f_{\vec{k}}(\epsilon - \mu)\vec{v}_{\vec{k}}, \tag{6}$$

where $\vec{v}_{\vec{k}}$ is the electron velocity and $f_{\vec{k}}$ is the electron distribution function which is obtained from the Boltzmann equation:

$$-\vec{v}_{\vec{k}}\cdot\frac{\partial f_{\vec{k}}}{\partial \vec{r}} - \frac{e}{\hbar}\left(\vec{E} + \frac{1}{c}\,\vec{v}_{\vec{k}}\times\vec{H}\right)\cdot\frac{\partial f_{\vec{k}}}{\partial \vec{k}}$$

$$= \frac{1}{4\pi^3}\int d\vec{k}'\,[f_{\vec{k}'}(1-f_{\vec{k}})\,Q(\vec{k}',\vec{k}) - f_{\vec{k}}(1-f_{\vec{k}'})Q(\vec{k},\vec{k}')]. \tag{7a}$$

When linearized, the Boltzmann equation can be written (for zero external electric and magnetic fields)

$$-v_x\left(\frac{\partial f^0_{\vec{k}}}{\partial \epsilon_{\vec{k}}}\right)\left(\frac{\epsilon-\mu}{k_B T}\right)$$

$$= -\frac{1}{4\pi^3}\,\frac{1}{k_B T}\int d\vec{k}'\,(\psi - \psi')\,P(\vec{k},\vec{k}') = W(\eta), \tag{7b}$$

where

$$f_{\vec{k}} = f^0_{\vec{k}} + k_B(-\nabla_x T)\eta, \tag{8a}$$

$$\eta = \left(-\frac{\partial f^0_{\vec{k}}}{\partial \epsilon_{\vec{k}}}\right)\psi, \tag{8b}$$

and

$$P(\vec{k},\vec{k}') = f^0_{\vec{k}}(1-f^0_{\vec{k}'})Q(\vec{k},\vec{k}').$$

$Q(\vec{k},\vec{k}')$ is the transition probability from state $\vec{k}$ to $\vec{k}'$, $f^0_{\vec{k}}$ is the equilibrium distribution function, and the temperature gradient is taken to be in the x direction.

The total scattering probability can always be written as the sum of the individual scattering probabilities. Here we consider two scattering mechanisms. If one of the scattering mechanisms can be described by a relaxation time τ, then the collision integral may be written

$$W(\eta) = -\eta/\tau + W'(\eta), \tag{9}$$

where $W'(\eta)$ is the collision integral for the second scattering process, one which cannot be described by a relaxation time. It should be noted that this does not amount to assuming Matthiessen's rule to be valid. If the scattering mechanism describable by a relaxation time is also the dominant one, then substituting Eqs. (8) and (9) into Eq. (7) and iterating yields η to zeroth and higher orders, namely,

$$\eta_0 = \left(-\frac{\partial f^0_{\vec{k}}}{\partial \epsilon_{\vec{k}}}\right)\left(\frac{\epsilon-\mu}{k_B T}\right)v_x\tau, \tag{10}$$

$$\eta_1 = \eta_0 + \tau W'(\eta_0), \tag{11}$$

$$\eta_2 = \eta_1 + \tau W'[\tau W'(\eta_0)]. \tag{12}$$

Substituting Eqs. (8a), (10), and (11) into Eq. (6) and noting that, for a crystal with cubic symmetry, $\kappa_e = J_Q/\nabla T$, one obtains

$$\kappa_e = \frac{1}{4\pi^3}\int d\vec{k}\left(-\frac{\partial f^0_{\vec{k}}}{\partial \epsilon_{\vec{k}}}\right)\frac{(\epsilon-\mu)^2}{T}\,v_x^2\tau$$

$$+\frac{1}{4\pi^3}\int d\vec{k}\,v_x\tau\,\frac{\epsilon-\mu}{k_B T}\,W'(\eta_0).$$

The first integral on the right-hand side is κ_τ, the thermal conductivity when only the dominant scattering mechanism is present. When both mechanisms are present (but $W_\tau = 1/\kappa_\tau$ is still dominant) it follows that

$$W_e = \frac{1}{\kappa_e} = W_\tau \left(1 - \frac{1}{4\pi^3 \kappa_\tau} \int d\vec{k}\, \frac{\epsilon - \mu}{k_B T}\, v_x \tau\, W'(\eta_0)\right)$$

$$= W_\tau + \frac{(1/4\pi^3) \int d\vec{k}\, \psi_0 [-W'(-\partial f_{\vec{k}}^0/\partial \epsilon_{\vec{k}}) \psi_0]}{|(1/4\pi^3) \int d\vec{k}\, k_B \psi_0 (\epsilon - \mu)(-\partial f_{\vec{k}}^0/\partial \epsilon_{\vec{k}})|^2} \quad (13)$$

The second term on the right-hand side is just the variational expression for the thermal resistivity if the first-order deviation function ψ_0 is identified as the trial function. $W'(\eta)$ is the collision integral for the other scattering mechanism. When the simple trial function, Eq. (1), is used to calculate W_τ, one readily obtains the Wiedemann–Franz law and thus $W_\tau T$ is independent of temperature.

Impurity scattering is generally considered to be isotropic and amenable to a relaxation-time approximation. For our very impure samples, we will assume that electron-impurity scattering is the dominant scattering mechanism and that it can be described by a relaxation time. Taking $W'(\eta_0)$ to be the electron-phonon collision integral and noting that the second term in Eq. (3) is just W_T, one observes that, in the impurity dominated case, Eq. (1) used as a trial function yields the temperature-dependent portion of the electronic thermal resistivity due to electron-phonon scattering. Thus, it is not surprising that the simple trial function (often called the impurity or "dirty-limit" trial function) yields calculated values that are in excellent quantitative agreement with the experimental results, as shown in Fig. 3(a). One expects calculations done using the impurity trial function [Eq. (1)] to become increasingly less accurate as electron-phonon scattering becomes more important because the impurity trial function becomes an increasingly poorer description of the real deviation function.

Figure 4(b) shows results for sample K – 9, the purest sample shown; at low temperatures the data lie 10–20% below the calculated values even when the corrected trial function, given by Eq. (2) is used. (This corrected trial function has no particular physical meaning but is merely an attempt to obtain lower values of the variational calculation.) Ekin[20] points out that below 4 K the corrected trial function yields a thermal resistivity that is estimated to be about 10% too high. This is insufficient to account for the observed difference.

This difference between theory and experiment should be contrasted with the electrical case, where calculations using the various pseudopotentials bracket the results for both pure and impure samples.[1] Except perhaps for the very impure samples, the thermal-resistance calculation is not as good as the electrical-resistance calculation. The correct pseudopotential should be the same for the electrical or thermal case; since the electrical calculation is very good, the pseudopotentials used should be reasonably accurate reflections of the true ion potentials. Hence the observed differences can probably be attributed to the choice of the trial function. The two most obvious possibilities in this regard are neglecting both phonon drag and any anisotropy in the electron distribution function. Roy and Wilkins[24] have calculated the effect of phonon drag on the electrical and thermal resistivity. They find that the magnitude of the phonon-phonon relaxation time is quite critical in establishing the drag resistance. However, when experimentally determined phonon-phonon relaxation times are used, the drag resistance turns out to be only a few tenths of a percent of the total resistance, negligible for the purposes of this discussion.

As the temperature is reduced, umklapp scattering will be confined to the areas of the Fermi surface nearest the zone boundaries (⟨110⟩ directions). Such localized (in momentum space) phonon scattering, similar to the so-called "hot spots" of Young,[25] could play a significant role in determining the transport properties of potassium. In particular, such localized scattering will create an anisotropic distribution function. The trial function used in the variational calculation should reflect this anisotropy. The effects of such an anisotropic distribution function have been calculated for the electrical resistivity.[26] In that case, the magnitude of the umklapp scattering contribution to the electrical resistivity is reduced by 10–15% while the normal component is unaffected. The umklapp contribution to the electrical resistivity exceeds that due to normal scattering by a factor of 4–5, whereas in the thermal resistivity both mechanisms contribute about equally in the 2–8 K temperature range. Thus it is likely that the effects of including an anisotropic trial function in a calculation of the thermal resistivity will be an order of magnitude less than in the electrical case, and therefore insufficient to account for the observed differences. Hence it appears that the difference between theory and experiment is not likely to be found in the gross approximations that have been made but rather in the more subtle behavior of the energy dependence of the trial function.

Referring again to Figs. 3 and 4, it is evident that, with the exception of the most impure samples, the measured thermal resistivity above 8 K does not change as rapidly as the calculated thermal resistivity. W_T/T^2 decreases more rapidly for impure specimens than for the pure specimens, but as discussed below, this behavior is due to lattice thermal conduction. Therefore, for all specimens the calculations seem to underestimate the high-temperature electronic thermal resistivity. Reasons for this are not clear. As far as the temperature dependence is concerned, electrical resistivity calculations yield excellent agreement with

the experimental results over the whole temperature range[1]; again, this indicates that the various pseudopotentials are not grossly incorrect. The main differences between the electrical and thermal resistivity are the roles of small angle and inelastic scattering. Pseudopotentials are generally considered to be quite good when used to calculate the effects of small angle scattering. Therefore, the energy dependence of the pseudopotential and the treatment of inelastic scattering appear to be possible explanations for the difference between the electrical and thermal cases. Yet another possibility may be related to the observed deviations from Matthiessen's rule.

The temperature-dependent portion of the measured thermal resistivity, which we have identified as W_T, will not be due entirely to electron-phonon scattering, but, as is shown below, can contain an additional temperature-dependent term. With only electron-impurity scattering present, the electrons, under the influence of a temperature gradient, will reach a steady-state distribution $f_{\vec{k}}^{\text{imp}}$. Similarly, with only electron-phonon scattering present, the steady-state distribution will be $f_{\vec{k}}^{\text{ph}}$. In general, $f_{\vec{k}}^{\text{ph}}$ will not be equal to $f_{\vec{k}}^{\text{imp}}$. When both types of scattering are present simultaneously, the resulting steady-state distribution will be a compromise between the two. The result of this is that when both mechanisms are present, the total resistivity is greater than the sum of the resistivities when each mechanism acts separately. Thus, the total resistivity can be written

$$W = W_{\text{imp}}(c) + W_{\text{ph}}(T) + \delta(c, T),$$

where $W_{\text{imp}}(c)$ and $W_{\text{ph}}(T)$ are, respectively, the impurity and phonon resistivities with each mechanism acting separately. $\delta(c, T)$, which can be shown to be always positive, can depend upon both the impurity concentration and the temperature. The variational calculation is done with a trial function that yields the best values of $W_{\text{ph}}(T)$, whereas the experimental data W_T contain the additional term $\delta(c, T)$. In the electrical case it is known that $\delta(c, T)$ can have a temperature dependence different than that of $W_{\text{ph}}(T)$.[27] $\delta(c, T)$ will be small at the lower temperatures but deviations from Matthiessen's rule might account for the observed difference between theory and experiment at the higher temperatures. In order to actually calculate a value for $\delta(c, T)$ with any degree of accuracy from experimental data the specimen geometrical factor must be very well known. In this experiment the geometrical factor is not known with sufficient accuracy so no attempts have been made to extract a value for $\delta(c, T)$ from our data.

We can, however, demonstrate deviations from Matthiessen's rule at *low* temperatures by comparing the coefficient B [see Eq. (14)] for samples of different purity. The purity dependence of B is shown in Fig. 5. (The estimated error is 5%.) The 50% change over this purity range is larger than the corresponding deviations (30%) observed in the electrical resistivity.[1] The curve drawn through the data points in Fig. 5 is only meant to indicate the general trend in the data; B is essentially constant in the low-purity range, decreases as the purity increases and then tends to become constant for high purities.

The present experiments show quite clearly that umklapp scattering plays an important role in determining the low-temperature thermal resistivity. However, the temperature dependence is not very much different from what one would expect if only normal scattering were present. Figure 1 of Ref. 20 shows the calculated thermal resistivity decomposed into the separate contributions due to normal and umklapp scattering. In the temperature interval from 4 to 7 K, umklapp scattering contributes as much as 50% to the total thermal resistivity. Even so, the total thermal resistivity is closely represented by a T^2 dependence. This should be contrasted with the electrical case where umklapp scattering contributes as much as 4 to 5 times the resistance of normal scattering in the same temperature range and the electrical resistivity cannot in any sense be described by a simple power law. It is a curious coincidence that just when the thermal resistivity due to the normal processes begins to deviate below a T^2 dependence, the resistivity due to umklapp processes increases in nearly the correct proportion to give a total thermal resistivity having a quadratic temperature dependence; this extends the regime over which the simple T^2 law appears valid.

This simple power-law behavior is best illustrated by displaying both the theory and experimental results in the more standard form shown in Figs. 6 and 7. The expression generally used to describe the electronic thermal resistivity of a metal is

$$W_e = A/T + BT^2. \tag{14}$$

Here BT^2 represents the electron-phonon scattering contribution to the resistivity, usually calculated using the Bloch theory and A/T is the thermal analog to the electrical residual resistivity; $A = \rho_0/L_0$, where ρ_0 is the electrical residual resistivity and L_0 is the Lorenz number. The results of calculations using the Bardeen pseudopotential and the uncorrected trial function are shown in Fig. 6. [These are the same results as the solid curve in Fig. 3(b).] This pseudopotential was chosen because it gives the greatest low-temperature curvature and therefore has the greatest deviations from a straight line on such a plot. The scale of the abscissa is the same as that used when plotting the

experimental data to obtain $(WT)_{T=0}$. Above 3 K, the theory is closely approximated by a straight line, but there is some upward curvature at the lower temperatures. Because of this, data should be taken to fairly low temperatures so that $(WT)_{T=0}$ can be determined accurately. In the less pure samples, the percentage error introduced by extrapolation from a high temperature will be small; however, it can be as large as 10% in the purer samples. (Note that the other pseudopotentials will give a much smaller curvature which represents a smaller possible extrapolation error.) Such an error will always overestimate the residual-resistivity ratio and can cause large errors in determining the temperature-dependent portion of the thermal resistivity. However, the percentage error in W_T will decrease with increasing temperature. Figure 7 shows the measured temperature dependence of the thermal resistance of potassium when plotted as WT vs T^3. The relevant specimen parameters as well as those parameters describing the curves [A and B, Eq. (14)] in this figure are listed in Table I. The residual-resistivity ratios listed in Table I have been obtained using the experimentally determined values for $(WT)_{T=0}$ and assuming the Wiedemann–Franz law to be valid. Values for B were determined from the data between 4 and 8 K. Both A and B are accurate to about 5%, the major error arising from the determination of the cross-sectional area.

To facilitate comparison with other work, the thermal conductivity as a function of temperature for representative samples is shown in Figs. 8 and 9. The solid curves in Figs. 8 and 9 are calculated from Eq. (14) using the experimentally determined values for A and B given in Table I. The dashed curve in Fig. 9 is computed in a similar manner except that the lattice conductivity, which is appreciable, has been included.[20]

Our results are in reasonable quantitative agreement with those of MacDonald, White, and Woods[10] whose measurements were done on potassium encapsulated in small glass capillaries. Differential thermal contraction will strain such potassium samples[23,28]; the resulting effects can introduce significant errors in the electrical resistivity and, presumably, in the thermal resistivity as well. Because of this, it does not seem reasonable to make any further comparisons with their data.

Our results are in considerable disagreement with those of Stauder and Mielczarek.[11] We see no evidence for any anomalous contributions to the thermal resistivity in any of the potassium samples that we have measured, whether pure or impure or in either single-crystal or polycrystalline form. (Samples K – 16 and K – 15 are in the same purity range as the single crystals measured by Stauder and Mielczarek.)

In an attempt to determine possible reasons for the differences between our measurements and those of Stauder and Mielczarek we have compared our experimental technique with theirs.[29] There exist a number of difficulties which we feel invalidate much of their data; several of them are listed below.

(i) Copper leads were used to make electrical connections to the thermometers. The low thermal resistance of such leads (about 0.01 Ω compared to our resistance of 3 Ω) gives poor isolation between the thermometers and the liquid-helium bath. Poor thermal isolation is particularly troublesome when the sample-to-thermometer thermal resistance is high as is likely when making contact to reactive materials such as potassium.

(ii) As far as we could determine, no attempt was made to compare their two germanium thermometers against one another or to take a zero-power-input temperature difference to use as a correction for small heat leaks and small thermometer calibration errors (see Sec. IID). They used commercial calibrations which are, in general, only accurate to 5 mK. When small applied temperature differences are used large errors in W will result. Note that our thermometers were both calibrated against the same standard.

(iii) They do not report any attempt to use their method to measure a metal such as indium of copper, whose thermal conductivity is known. If such measurements had been made, under the same experimental conditions as used for potassium, and the apparatus shown to perform properly, then doubts raised by the first two possibilities might be eliminated.

In the absence of any such calibration measurements and in view of the problems raised above we must conclude that the anomalous results reported by Stauder and Mielczarek are not a property of potassium.

Figure 10 shows the calculated lattice thermal conductivity of potassium as a function of the temperature.[20] The lattice conductivity values in Fig. 10 were calculated by Ekin assuming only phonon-electron scattering; phonon-impurity scattering has been neglected. Archibald, Dunick, and Jericho[30] have measured the lattice thermal conductivity of extremely impure potassium-cesium alloys. When their results are compared with theory, phonon-impurity scattering is found to be quite important. Our "dirty" samples are an order of magnitude more pure than any of their specimens so such scattering will be much less important. However, phonon-impurity scattering will increase with temperature. Thus the calculated thermal conductivity plotted in Fig. 10 should be regarded as an upper limit, particularly at the higher temperatures.

The heat current carried by the lattice will be

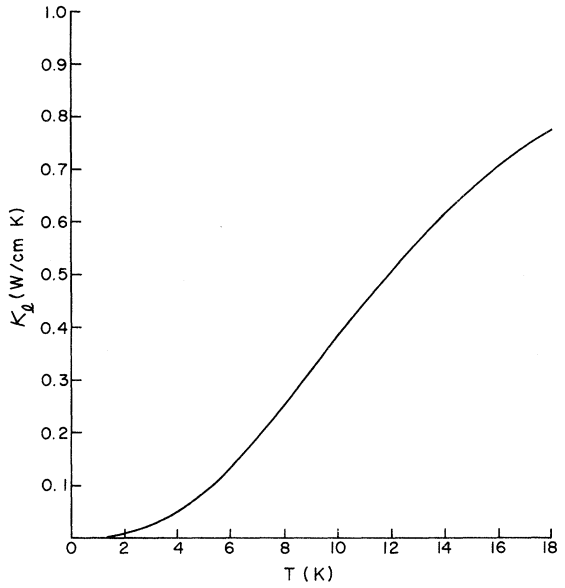

FIG. 10. Theoretical lattice thermal conductivity as a function of temperature (from Ref. 20).

added to the electronic heat current; therefore, when lattice conduction cannot be neglected, the measured thermal resistance will be less than the resistance due to electronic conduction alone. Comparing the curve in Fig. 10 with those in Figs. 8 and 9, one sees that below about 6 K the lattice term can be neglected in all but the most impure specimen. For reasonably pure specimens (residual-resistivity ratio ≥ 2000), the calculated lattice conduction is less than 1% of the total conduction at 6 K. At higher temperatures the lattice becomes more important. Above 20 K, the lattice can account for as much as 50% of the heat conduction depending on purity. However, for impure samples the lattice conductivity may be very important at lower temperatures. For example, in sample K–16, having a residual resistivity ratio of 195, lattice conduction accounts for about 13% of the total heat conduction at 10 K. The lower curve in Fig. 9 represents a fit to Eq. (14) where A and B are determined from the data below 6 K. If the lattice conductivity given in Fig. 10 is simply added to the conductivity given by Eq. (14), one obtains the upper curve in Fig. 9. It is quite evident that the correction is larger at the higher temperatures. As the purity decreases, lattice conduction becomes an increasingly larger fraction of the total conduction. As previously mentioned this is responsible for the decrease in W_T/T^2 for the more impure samples being more rapid than in the purer specimens above 8 K. (No corrections for the lattice conductivity have been made for the calculated curves shown in Fig. 8.)

IV. CONCLUSION

We have presented evidence showing that the low-temperature thermal resistivity of potassium can be adequately explained using semiclassical ideas. The importance of umklapp scattering has been demonstrated. Umklapp processes become important between 2 and 3 K and eventually become responsible for about 50% of the total thermal resistivity. However, the temperature dependence of the normal and umklapp contributions to the thermal resistivity complement one another in a manner that results in an apparent T^2 law for the total thermal resistivity to temperatures greater than $\frac{1}{10}\Theta_D$.

Detailed comparison between theory and experiment shows that the agreement is better at low than at high temperatures. The fairly large observed deviations from Matthiessen's rule might be responsible for the disagreement at high temperatures and it would be useful to attempt to include both electron-phonon and electron-impurity scattering in the variational calculation to see how this affects the temperature dependence of the thermal resistivity.

No anomalous electron or phonon contributions to the thermal resistivity are observed. The effects of lattice conductivity are clearly present even in samples of intermediate purity; this additional conduction mechanism must be taken into account if accurate comparisons with theory are to be made. The existence of a sizable lattice conductivity in even reasonably pure samples makes the thermal resistivity a much more difficult transport property to analyze than the electrical resistivity.

ACKNOWLEDGMENTS

We are grateful for many useful and stimulating discussions with N. W. Ashcroft, J. W. Ekin, J. W. Wilkins, and R. Bowers. Special thanks are extended to D. K. Wagner for his many useful comments and critical reading of this manuscript. C. H. Stephan developed much of the experimental system used in this study in connection with an earlier magnetothermal project; we have benefited extensively from both his efforts and experience.

---

†Work supported partly by the U. S. Atomic Energy Commission under Contract No. AT(11-1)-3150, Tech. Rept. No. COO-3150-5 and partly by the Advanced Research Projects Agency through the Materials Science Center at Cornell University, MSC Report No. 1842.

*Alfred P. Sloan Research Fellow.

[1]J. W. Ekin and B. W. Maxfield, Phys. Rev. B 4, 4215 (1971); J. W. Ekin, Phys. Rev. Lett. 26, 1550 (1971); P. N. Trofimenkoff and J. W. Ekin, Phys. Rev. B 4, 2392 (1971).

[2]H. Taub, R. L. Schmidt, B. W. Maxfield, and R. Bowers, Phys. Rev. B 4, 1134 (1971).
[3]D. Gugan, Proc. Roy. Soc. (London) A325, 223 (1971).
[4]J. Schaefer and J. Marcus, Phys. Rev. Lett. 27, 535 (1971).
[5]J. Lass, J. Phys. C 3, 1926 (1970).
[6]B. K. Jones, Phys. Rev. 179, 637 (1969).
[7]P. A. Penz and R. Bowers, Phys. Rev. 172, 991 (1968).
[8]D. Shoenberg and P. J. Stiles, Proc. Roy. Soc. A281, 62 (1964); M. J. G. Lee and L. M. Falicov, Proc. Roy. Soc. A304, 319 (1968).
[9]It should be noted that A. Overhauser has discussed the possibility of a two-sheet Fermi surface for potassium. See for example, A. W. Overhauser, Phys. Rev. 167, 691 (1968); A. W. Overhauser, Phys. Rev. Lett. 27, 938 (1971).
[10]D. K. C. MacDonald, G. K. White, and S. B. Woods, Proc. Roy. Soc. (London) A235, 358 (1956).
[11]R. F. Stauder and E. V. Mielczarek, Phys. Rev. 158, 630 (1967).
[12]Silicone Vacuum Grease, Dow-Corning Co., Midland, Mich.
[13]C. H. Stephan and B. W. Maxfield, Phys. Rev. B 6, 2893 (1972).
[14]It should be noted that much better multichannel scanners are now available. A reed relay scanner would have eliminated much of this noise problem.
[15]DC-200 Fluid, Dow-Corning Co., Midland, Mich.
[16]The following is a list of the various oils and greases that were tried: Silicone Grease, Dow-Corning Co.; Apiezon L, M, N, and T grease and J-oil, J. G. Biddle Co.; Cry-Con Grease, Air Products Co.; 504 diffusion pump oil, Dow-Corning Co.
[17]J. H. McTaggart and G. A. Slack, Cryogenics 9, 384 (1969).
[18]Obtained from Cryocal, Inc., Riviera Beach, Fla.
[19]J. D. Filby and D. L. Martin, Proc. Roy. Soc. (London) A284, 83 (1964).
[20]J. W. Ekin, Phys. Rev. B 6, 371 (1972).
[21]This argument parallels a similar calculation for the electrical resistivity by D. K. Wagner, Ph. D. thesis (Cornell University, 1972) (unpublished).
[22]For example, see J. M. Ziman, *Electrons and Phonons* (Oxford U. P., London, 1960).
[23]We define the residual-resistivity ratio, RRR $=\rho(300\,\mathrm{K})/\rho(0\,\mathrm{K})$, and use a room-temperature resistivity of 7.19 $\mu\Omega$ cm after J. S. Dugdale and D. Gugan, Proc. Roy. Soc. A270, 186 (1962).
[24]M. Roy and J. W. Wilkins (private communication).
[25]R. A. Young, Phys. Rev. 175, 813 (1968).
[26]J. W. Ekin (private communication).
[27]J. Bass, Adv. Phys. 21, 431 (1972) (a review paper on deviations from Matthiessen's rule).
[28]J. S. Dugdale and D. Gugan, J. Sci. Instru. 40, 28 (1963).
[29]R. F. Stauder, Ph. D. thesis (Catholic University, 1968) (unpublished).
[30]M. A. Archibald, J. E. Dunick, and M. H. Jericho, Phys. Rev. 153, 786 (1967).

PHYSICAL REVIEW B VOLUME 7, NUMBER 4 15 FEBRUARY 1973

Chemically Motivated Pseudopotential for Sodium*

William C. Topp
Department of Chemistry, Princeton University, Princeton, New Jersey 08540

John J. Hopfield
Department of Physics, Princeton University, Princeton, New Jersey 08540

(Received 24 May 1972)

A local pseudopotential of the form $V=V_0\cos kr+C$, $r<r_c$, $V=-1/r$, $r>r_c$, is used to fit the experimental ground-state energy of atomic sodium. This form is chosen so as to mirror as closely as possible the actual valence charge distribution of Na. This is important in the calculation of chemical properties such as bonding and cohesion. Electrostatic calculations of the cohesive energy of the bcc metal from the virial theorem and from the electrostatic self-energy of the lattice are performed and the results compared. The results bear on the accuracy of electron-gas calculations in metals and the techniques of pseudopotential calculations. The phonon spectrum is calculated and all results are compared to those obtained with a Shaw-type flat-bottom pseudopotential.

I. INTRODUCTION

Pseudopotential theory has proven to be of great use both to experimentalists, as a framework within which to report their results, and to theoreticians, as a computationally facile way to approach solid-state calculations. By far the most extensive applications of the theory have been to the calculation of the one-electron properties of solids in a nearly-free-electron viewpoint. Previous pseudopotentials have been designed to reproduce the optical spectrum of the solid or the energy levels of the atom. Little attention has been given to the importance of matching the correct charge distribution as well. We present here several calculations with a potential that models not only the atomic energy levels but also the valence charge distribution. The purpose of this choice is the cal-